

Temporal Graph Kernels for Classifying Dissemination Processes

Lutz Oettershagen* Nils M. Kriege† Christopher Morris† Petra Mutzel*

Abstract

Many real-world graphs or networks are temporal, e.g., in a social network persons only interact at specific points in time. This information directs *dissemination processes* on the network, such as the spread of rumors, fake news, or diseases. However, the current state-of-the-art methods for supervised graph classification are designed mainly for static graphs and may not be able to capture temporal information. Hence, they are not powerful enough to distinguish between graphs modeling different dissemination processes. To address this, we introduce a framework to lift standard graph kernels to the temporal domain. Specifically, we explore three different approaches and investigate the trade-offs between loss of temporal information and efficiency. Moreover, to handle large-scale graphs, we propose stochastic variants of our kernels with provable approximation guarantees. We evaluate our methods on a wide range of real-world social networks. Our methods beat static kernels by a large margin in terms of accuracy while still being scalable to large graphs and data sets. Hence, we confirm that taking temporal information into account is crucial for the successful classification of dissemination processes.

Keywords— Temporal graphs, Classification, Kernels

1 Introduction

Linked data arise in various domains, e.g., in chem- and bioinformatics, social network analysis and computer vision, and can be naturally represented as graphs. Therefore, machine learning with graphs has become an active research area of increasing importance. A prominent method primarily used for supervised graph classification with support vector machines are *graph kernels*, which compute a similarity score between pairs of graphs. In the last fifteen years, a plethora of graph kernels has been published [17]. With few exceptions, these are designed for static graphs and cannot utilize temporal information. However, real-world graphs often have temporal information attached to the edges, e.g., modeling times of interaction in a social network, which directs any dissemination process, i.e., the spread of

information over time, in the temporal graph. Consider, for example, a social network where persons A and B were in contact before persons B and C became in contact. Consequently, information may have been passed from persons A to C but not vice versa. Hence, whenever such implicit direction is essential for the learning task, static graph kernels will inevitably fail.

To further exemplify this, assume that a (sub-)group in a social network suffers from un-specific symptoms, that occurred at some point in time and are probably caused by a disease. Here, nodes represent persons, and the edges represent contacts between them at certain points in time, cf. Figure 1. An obvious question now is whether an infectious disease causes the symptoms. However, dissemination processes are typically complex, since persons may have different risk factors of becoming infected, the transmission rate is unknown and, finally, the network structure itself might suffer from noise. Therefore, this question is difficult to answer by just analyzing a single network. But, assume that similar network data of past epidemics is available. Hence, we can model the detection of dissemination process of a disease as a supervised graph classification problem. In the simplest case, one class contains graphs under a dissemination process of a disease and the other class consists of graphs, where the node labels cannot be explained by the temporal information. Furthermore, notice that infections, or disseminated information in general, often may not be recognized or not reported [36]. Therefore, we additionally consider the scenario where disseminated information is incomplete. Finally, observe that the above learning problem can also model the detection of other dissemination processes in networks, e.g., dissemination of fake news in social media [34] or viruses in computer or mobile phone networks [1].

The key to solving these classification tasks are methods that adequately take the temporal characteristics of such graphs into account. We consider *temporal graphs*, where edges exist at specific points in time and node labels, e.g., representing infected and non-infected, may change over time.

1.1 Contributions We propose graph kernels for classifying dissemination processes in temporal graphs.

*Institute of Computer Science I, University of Bonn, {lutz.oettershagen, petra.mutzel}@cs.uni-bonn.de.

†Department of Computer Science, TU Dortmund University, {nils.kriege, christopher.morris}@tu-dortmund.de.

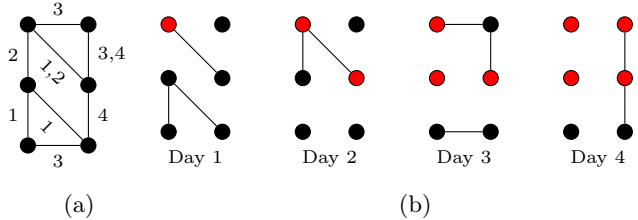


Figure 1: Example of an epidemic outbreak: (a) A temporal graph where the vertices represent persons and edges their interaction. (b) For each day t there is a static graph containing only the edges existing on day t . Infected vertices are labeled red.

More specifically, our main contributions are:

1. We introduce three different techniques to map temporal graphs to static graphs such that conventional, static kernels can be successfully applied. For all three approaches, we analyze the trade-offs between loss of temporal information and size of the transformed graph.
2. For large-scale problems, we present a stochastic kernel directly based on temporal walks with provable approximation guarantees.
3. We comprehensively evaluate our methods using real-world data sets with simulations of epidemic spread. Our results confirm that taking temporal information into account is crucial for the detection of dissemination processes.

1.2 Related Work Graph kernels have been studied extensively in the past 15 years, see [17]. Almost all kernels focus on static graphs. Important approaches include random-walk and shortest paths based kernels [7, 31, 4, 18], as well as the Weisfeiler-Lehman subtree kernel [30, 23]. Further recent works focus on assignment-based approaches [16, 27], spectral approaches [15], and graph decomposition approaches [26].

There has been some work considering dynamic graphs. In [20] a family of algorithms to recompute the random walk kernel efficiently when graphs are modified is presented. Wu et al. [37] propose graph kernels for human action recognition in video sequences. To this end, they encode the features of each frame as well as the dynamic changes between successive frames by separate graphs, which are then compared by random walk kernels. Paaßen et al. [28] use graph kernels for predicting the next graph in a dynamically changing series of graphs. Using a similar setting, Anil et al. [2] propose spectral graph kernels to predict the evolution of social networks. General spatio-temporal convolution kernels for trajectory data of simultaneously moving objects were introduced in [14]. Wang et al. [35] study the classification of temporal graphs in which both

vertex and edge sets can change over time. Here, information propagation is considered as a sequence of individual graphs, where the number of vertices is increasing when an information outburst occurs. They aim to identify such outbursts of information propagation. However, to the best of our knowledge, no graph kernels have been suggested that take temporality of edges and labels, as well as dissemination processes on graphs into account.

An extensive overview of temporal graphs, their static representations, and temporal walks can be found in [12, 21]. In [25] temporal random walks are used to obtain node embeddings for link prediction in evolving networks. In [9], the Katz centrality is extended to temporal graphs using temporal walks. Holme [11] examines how temporal graphs can be used for epidemiological models. The author evaluates different static representations of temporal graphs by comparing predicted and simulated epidemic outbreak sizes.

Identifying vertices that play an important role in dissemination processes has also been studied. For example, Leskovec et al. [19] study the problem of placing sensors in a water distribution network to quickly detect contaminants. Recently, methods for dynamic graphs were proposed where edges may be added to the graph as time progresses. All of these approaches focus on link prediction in single graphs, see, e.g., [25, 32]. Graph neural networks [8] emerged as an alternative for graph classification. Our new approaches can be combined with neural architectures, e.g., see [24].

2 Preliminaries

A *labeled, undirected (static) graph* $G = (V, E, l)$ consists of a finite set of vertices V , a finite set $E \subseteq \{\{u, v\} \subseteq V \mid u \neq v\}$ of undirected edges, and a labeling function $l: V \cup E \rightarrow \Sigma$ that assigns a label to each vertex or edge, where Σ is a finite alphabet. In a labeled, *directed* graph $E \subseteq \{(u, v) \in V \times V \mid u \neq v\}$. We use $V(G)$ to denote the set of vertices of G . A (static) *walk* in a graph G is an alternating sequence of vertices and edges connecting consecutive vertices. For notational convenience we sometimes omit edges. The length of a walk $(v_1, v_2, \dots, v_{k+1})$ is k .

A *labeled, undirected, temporal graph* $\mathbf{G} = (V, \mathbf{E}, l)$ consists of a finite set of vertices V , a finite set \mathbf{E} of undirected *temporal edges* $e = (\{u, v\}, t)$ with u and v in V , $u \neq v$, *availability time* (or *time stamp*) $t \in \mathbb{N}$, and a labeling function. Here the labeling function $l: V \times T \rightarrow \Sigma$ assigns a label to each vertex at each time step $t \in T = \{1, \dots, t_{\max} + 1\}$ with t_{\max} being the largest time stamp of any $e \in \mathbf{E}$. Note that for a temporal graph the number of edges is not polynomially bounded by the number of vertices. For $v \in V$ let $T(v)$

be the set of availability times of edges incident to v . For convenience, we regard the set of availability times as a sequence that is ordered by the canonical ordering on the natural numbers. The bijection $\tau_v: T(v) \rightarrow \{1, \dots, |T(v)|\}$ assigns to each time its position in the ordered sequence of $T(v)$ for $v \in V$. The degree $d(v)$ of a vertex v in a temporal graph is the sum of the numbers of edges incident to v over all time steps.

2.1 Kernels for Static Graphs A *kernel* on a non-empty set \mathcal{X} is a positive semidefinite function $\kappa: \mathcal{X} \times \mathcal{X} \rightarrow \mathbb{R}$. Equivalently, a function κ is a kernel if there is a *feature map* $\phi: \mathcal{X} \rightarrow \mathcal{H}$ to a Hilbert space \mathcal{H} with inner product $\langle \cdot, \cdot \rangle$, such that $\kappa(x, y) = \langle \phi(x), \phi(y) \rangle$ for all x and y in \mathcal{X} . Let \mathcal{G} be the set of all graphs, then a function $\mathcal{G} \times \mathcal{G} \rightarrow \mathbb{R}$ is a *graph kernel*. We briefly summarize two well-known kernels for static graphs.

Random walk kernels measure the similarity of two graphs by counting their (weighted) common walks [7, 31]. For a walk $w = (v_1, e_1, \dots, v_{k+1})$ let $L(w) = (l(v_1), l(e_1), \dots, l(v_{k+1}))$ denote the labels encountered on the walk. Two walks w_1 and w_2 are considered to be common if $L(w_1) = L(w_2)$. We consider the k -step random walk kernel $\kappa_{\text{RW}}^k(G, H) = \langle \phi_{\text{RW}}(G), \phi_{\text{RW}}(H) \rangle$ counting walks up to length k . Here, the feature map ϕ_{RW} is defined by $\phi_{\text{RW}}(G)_s = |\{w \in \mathcal{W}_\ell(G) \mid s = L(w)\}|$, where $s \in \Sigma^{2\ell+1}$ and $\mathcal{W}_\ell(G)$ is the set of walks in G of length $\ell \in \{0, \dots, k\}$.

Weisfeiler–Lehman subtree kernels are based on the well-known *color refinement algorithm* for isomorphism testing [30]: Let G and H be graphs, and l be a labeling function $V(G) \cup V(H) \rightarrow \Sigma$. In each iteration $i \geq 0$, the algorithm computes a labeling function $l^i: V(G) \cup V(H) \rightarrow \Sigma$, where $l^0 = l$. Now in iteration $i > 0$, we set $l^i(v) = (l^{i-1}(v), \{\{l^{i-1}(u) \mid u \in N(v)\}\})$ for v in $V(G) \cup V(H)$. In practice, one maps the above pair to a unique element from Σ . The idea of the *Weisfeiler–Lehman subtree kernel* [30] is to compute the above algorithm for $h \geq 0$ iterations and after each iteration i compute a feature map $\phi^i(G)$ in $\mathbb{R}^{|\Sigma^i|}$ for each graph G , where $\Sigma_i \subseteq \Sigma$ denotes the image of l^i . Each component $\phi^i(G)_c$ counts the number of occurrences of vertices labeled with c in Σ_i . The overall feature map $\phi_{\text{WL}}(G)$ is defined as the concatenation of the feature maps of all h iterations. Then, the Weisfeiler–Lehman subtree kernel for h iterations is $\kappa_{\text{WL}}^h(G, H) = \langle \phi_{\text{WL}}(G), \phi_{\text{WL}}(H) \rangle$. This kernel can also be interpreted in terms of walks. A label $l^i(v)$ represents the unique rooted tree of height i obtained by simultaneously taking all possible walks of length i starting at v , where repeated vertices visited in the past are treated as distinct.

3 A Framework for Temporal Graph Kernels

In the following temporal graphs are mapped to a static graphs such that conventional static kernels can be applied, e.g., the random walk or Weisfeiler–Lehman subtree kernel. To catch temporal information, we use *temporal walks*, which are time respecting walks. That is, the traversed edges along a temporal walk have strictly increasing availability times. We assume that traversing an edge in a temporal walk does need one unit of time and is not possible instantaneously.

DEFINITION 1. A temporal walk of length ℓ is an alternating sequence of vertices and temporal edges $(v_1, e_1 = (\{v_1, v_2\}, t_1), v_2, \dots, e_\ell = (\{v_\ell, v_{\ell+1}\}, t_\ell), v_{\ell+1})$ such that $t_i < t_{i+1}$ for $1 \leq i < \ell$. For a temporal walk the waiting time at vertex v_i with $1 < i \leq \ell$ is $t_i - (t_{i-1} + 1)$. The set of temporal walks (of length ℓ) in a temporal graph \mathbf{G} is denoted by $\mathcal{W}^{\text{tmp}}(\mathbf{G})$ ($\mathcal{W}_\ell^{\text{tmp}}(\mathbf{G})$). Finally, we define the function L that maps a temporal walk w to the label sequence $L(w) = (l(v_1, t_1), l(v_2, t_1 + 1), l(v_2, t_2), l(v_3, t_2 + 1), \dots, l(v_\ell, t_\ell), l(v_{\ell+1}, t_\ell + 1))$.

Temporal walks enable us to gain insights into the interpretation of the derived temporal graph kernels whenever the static graph kernel can be understood in terms of walks. This is natural in the case of random walk kernels, but also for the widely-used Weisfeiler–Lehman subtree kernel, cf. Section 2.1. We introduce three approaches, that differ in the size of the resulting static graph and in their ability to preserve temporal information as well as to model waiting times, see Table 1 for an overview.

3.1 Reduced Graph Representation First, we propose a straight-forward approach to incorporate temporal information in static graphs. In a temporal graph $\mathbf{G} = (V, \mathbf{E}, l)$ a pair of vertices may be connected with multiple edges each with a different availability time. In this case, we only preserve the edge with the earliest availability time and delete all other edges. We obtain the subgraph $\mathbf{G}' = (V, \mathbf{E}', l)$ with $\mathbf{E}' \subseteq \mathbf{E}$. From this we construct a static, labeled, undirected graph $RG(\mathbf{G}) = (V, E, l_s)$ by inserting an edge $e = \{u, v\}$ into E for every temporal edge $e' = (\{u, v\}, t') \in \mathbf{E}'$. We set the new static edge labels $l_s(e)$ to the number of the position $\tau(t')$ in the ordered sequence of all (remaining) availability times t' in \mathbf{E}' . Next, the temporal development of the dissemination is encoded using the vertex labels. Therefore, if the label of a vertex $v \in V$ in \mathbf{G} stays constant over time, we set $l_s(v) = 0$. For the remaining vertex labels we take the ordered sequence T_V of all points in time when any vertex label changes for the first time. Then, for each vertex changing its label for the first time at time t_i , we set $l_s(v) = \tau(t_i)$, where

Table 1: Overview of the trade-offs of the proposed transformations. The third column describes the ability of the approaches to take waiting times into account: \times not supported, \star always, \checkmark approach is flexible.

Transformation	Preserves information	Waiting times	Size of static graph
Reduced Graph Representation	\times	\times	$\mathcal{O}(V ^2)$
Directed Line Graph Expansion	\checkmark	\checkmark	$\mathcal{O}(\mathbf{E} ^2)$
Static Expansion	\checkmark	\star	$\mathcal{O}(\mathbf{E})$

$\tau(t_i)$ denotes the position of t_i in the sequence T_V .

Applying this procedure results in the reduced graph representation $RG(\mathbf{G}) = (V, E, l_s)$. Clearly, the transformation may lead to a loss of information. However, notice that $RG(\mathbf{G})$ is a simple, undirected graph with at most one edge between each pair of vertices. Hence, its number of edges is bounded by $|V|^2$, which can be much smaller than $|\mathbf{E}|$.

3.2 Directed Line Graph Expansion In order to avoid a loss of information, we propose to represent temporal graphs by directed static graphs that are capable of fully encoding temporal information.

DEFINITION 2. (DIRECTED LINE GRAPH EXPANSION) Given a temporal graph $\mathbf{G} = (V, \mathbf{E}, l)$, the directed line graph expansion $DL(\mathbf{G}) = (V', E', l')$ is the directed graph, where every temporal edge $(\{u, v\}, t)$ is represented by two vertices n_{uv}^t and n_{vu}^t , and there is an edge from n_{uv}^t to n_{xy}^s if $v = x$ and $t < s$. For each vertex n_{uv}^t , we set the label $l'(n_{uv}^t) = (l(u, t), l(v, t + 1))$.

Figure 2b shows an example of the transformation for the graph shown in Figure 2a. The following lemma relates temporal walks in a temporal graph and the static walks in its directed line graph expansion.

PROPOSITION 3.1. Let \mathbf{G} be a temporal graph and $\ell \geq 0$. The walks in $\mathcal{W}_\ell(DL(\mathbf{G}))$ are in one-to-one correspondence with the temporal walks in $\mathcal{W}_{\ell+1}^{tmp}(\mathbf{G})$.

Proof. Let $(v_1, (\{v_1, v_2\}, t_1), v_2, \dots, (\{v_\ell, v_{\ell+1}\}, t_\ell), v_{\ell+1})$ be a temporal walk of length $\ell \geq 2$ in \mathbf{G} . Then $(n_{v_1 v_2}^{t_1}, n_{v_2 v_3}^{t_2}, \dots, n_{v_\ell v_{\ell+1}}^{t_\ell})$ is a walk of length $\ell - 1$ in $DL(\mathbf{G})$, since the vertices represent temporal edges of \mathbf{G} that are consecutively connected by directed edges in $DL(\mathbf{G})$ provided that $t_i < t_{i+1}$ for $i \in \{1, \dots, \ell - 1\}$. This holds for every temporal walk.

Vice versa, let $(n_{v_1 v_2}^{t_1}, n_{v_2 v_3}^{t_2}, \dots, n_{v_\ell v_{\ell+1}}^{t_\ell})$ be a walk in $DL(\mathbf{G})$. Due to the construction of $DL(\mathbf{G})$ the time stamps satisfy $t_1 < t_2 < \dots < t_\ell$ and we can construct a unique temporal walk in \mathbf{G} from the sequence of vertices as above. \square

Note that for $\ell = 0$ the two vertices n_{uv}^t and n_{vu}^t representing the same temporal edge $(\{u, v\}, t)$ correspond to

two different temporal walks traversing the edge in different directions. In Figure 2b the walk $(n_{ca}^2, n_{ab}^3, n_{bc}^7)$ in $DL(\mathbf{G})$ of length 2 corresponds to the temporal walk $(c, (\{c, a\}, 2), a, (\{a, b\}, 3), b, (\{b, c\}, 7), c)$ of length 3 in the temporal graph \mathbf{G} .

The vertex labeling of $DL(\mathbf{G})$ is sufficient to encode all the label information of the temporal graph \mathbf{G} , i.e., two temporal walks exhibit the same label sequence (according to the function L in Definition 1) if and only if the corresponding walks in the directed line graph expansion have the same label sequence. Therefore, all static kernels that can be interpreted in terms of walks are lifted to temporal graphs and the concept of temporal walks by applying them to the directed line graph expansion. Moreover, the directed line graph expansion supports to take waiting times into account by annotating an edge (n_{uv}^s, n_{vu}^t) with the waiting time $t - s - 1$ at v . We proceed by studying basic structural properties of the directed line graph expansion.

PROPOSITION 3.2. Let $\mathbf{G} = (V, \mathbf{E})$ be a temporal graph and $DL(\mathbf{G}) = (V', E')$ its directed line graph expansion. Then, $|V'| = 2|\mathbf{E}|$ and

$$|E'| \leq -|\mathbf{E}| + \frac{1}{2} \sum_{v \in V} d^2(v) = \mathcal{O}(|\mathbf{E}|^2),$$

where $d(v)$ denotes the degree of v in \mathbf{G} .

Proof. The number of vertices directly follows from the construction. The directed line graph expansion $DL(\mathbf{G})$ of the temporal graph \mathbf{G} is closely related to the classical directed line graph of a modified copy of \mathbf{G} obtained by deleting all time stamps (leading to indistinguishable parallel edges) and replacing all undirected edges by two directed copies. We use the following classical result [10]. For a directed graph $G = (V, E)$ the number of edges in the directed line graph is $\sum_{v \in V} d^-(v) \cdot d^+(v)$, where $d^-(v)$ is the in- and $d^+(v)$ the outdegree of v . After replacing all undirected edges by two directed copies the in- and outdegrees are equal for each vertex. Furthermore, the directed line graph expansion of \mathbf{G} has at most half the edges, because for the vertices n_{uv}^t , n_{vu}^s and n_{wb}^t , n_{bw}^s at most one time constraint $s < t$ or $s > t$ can be satisfied. Finally, between n_{uv}^t and n_{wb}^t there is no edge, therefore we subtract $|\mathbf{E}|$ and the result follows. \square

Since a cycle in the directed line graph expansion would correspond to a cyclic sequence of edges with strictly increasing time stamps, the directed line graph $DL(\mathbf{G})$ of a temporal graph \mathbf{G} is acyclic. Consequently, the maximum length of a walk in the directed line graph expansion is bounded. Therefore, there is no need to down-weight walks with increasing length to ensure convergence, which avoids the problem of *halting* [31].

3.3 Static Expansion Kernel A disadvantage of the directed line graph expansion is that it may lead to a quadratic blowup w.r.t. the number of temporal edges. Here, we propose an approach that utilizes the *static expansion* of a temporal graph resulting in a static graph of linear size. The static expansion $SE(\mathbf{G})$ of a temporal graph \mathbf{G} is a static, directed and acyclic graph that contains the temporal information of \mathbf{G} . Similar approaches for static expansions have been used to solve a variety of problems on temporal graphs, see, e.g., [22].

For $\mathbf{G} = (V, \mathbf{E}, l)$ we construct $SE(\mathbf{G}) = (U, E, l')$ with U being a set of *time-vertices*. Each time-vertex $(v, t) \in U$ represents a vertex $v \in V$ at time t . Time-vertices are connected by directed edges that mirror the flow of time, i.e., if an edge from $(v, t) \in U$ to $(u, s) \in U$ exists, then $t < s$. Because edges in \mathbf{E} are non-directed, the transformation has to consider both possible directions. It follows, that for each temporal edge $e \in \mathbf{E}$, we introduce at most four time-vertices that represent the start and end points of e . Next, we add edges that correspond to temporal edges in \mathbf{E} , and additional edges that represent possible waiting times at a vertex.

DEFINITION 3. (STATIC EXPANSION) For a temporal graph $\mathbf{G} = (V, \mathbf{E}, l)$, we define the static expansion as a labeled, directed graph $SE(\mathbf{G}) = (U, E, l')$, with vertex set $U = \{(u, t), (v, t), (u, t + 1), (v, t + 1) \mid (\{u, v\}, t) \in \mathbf{E}\}$, and edge set $E = E_N \cup E_{W_1} \cup E_{W_2}$, where

$$E_N = \{((u, t), (v, t + 1)), ((v, t), (u, t + 1)) \mid (\{u, v\}, t) \in \mathbf{E}\},$$

$$E_{W_1} = \{((w, i + 1), (w, j)) \mid (w, i + 1), (w, j) \in U, i, j \in T(w), \tau_w(i) + 1 = \tau_w(j) \text{ and } i + 1 < j\}, \text{ and}$$

$$E_{W_2} = \{((w, i), (w, j)) \mid (w, i), (w, j) \in U, i, j \in T(w), \tau_w(i) + 1 = \tau_w(j) \text{ and } i < j\}.$$

For each time-vertex $(w, t) \in U$, we set $l'((w, t)) = l(w, t)$. For each edge in $e \in E_N$, we set $l'(e) = \eta$, and for each edge in $e \in E_{W_1} \cup E_{W_2}$, we set $l'(e) = \omega$.

Figure 2c shows an example of the transformation. Notice that the label sequence of a static walk in $SE(\mathbf{G})$ encodes the times of waiting. Since for all edges

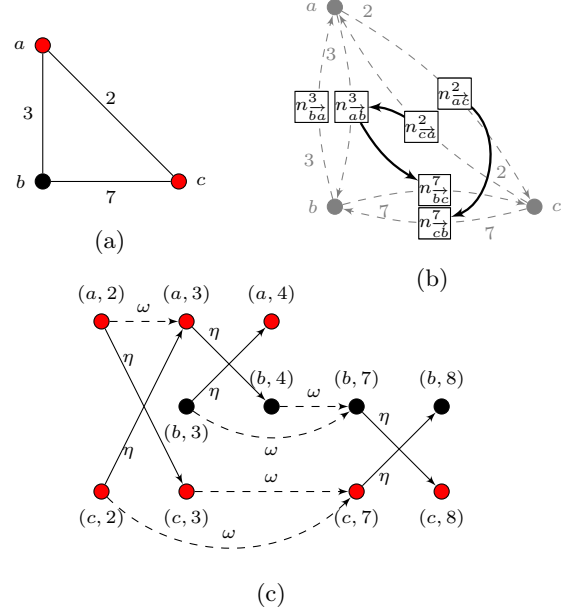


Figure 2: (a) A temporal graph \mathbf{G} with (static) red and black vertex labels. (b) Directed line graph expansion $DL(\mathbf{G})$ (edges are in solid and vertex labels are omitted) (c) Static expansion $SE(\mathbf{G})$.

$((u, t_1), (v, t_2)) \in E$ it holds that $t_1 < t_2$, the resulting graph is acyclic. Finally, we have the following result.

PROPOSITION 3.3. *The size of the static expansion $SE(\mathbf{G}) = (U, E, l')$ of a temporal graph \mathbf{G} is in $\mathcal{O}(|\mathbf{E}|)$.*

Proof. The size of U is bounded by $4 \cdot |\mathbf{E}|$, because at most four vertices for each temporal edge $e \in \mathbf{E}$ are inserted. For each $e \in \mathbf{E}$, there are at most six edges in E . Two edges that represent using e at time t and four possible waiting edges, one at each vertex inserted for edge e . Consequently, $|E| \in \mathcal{O}(|\mathbf{E}|)$. \square

4 Approximation for the directed line graph representation

Although the directed line graph representation preserves the temporal information and is able to model waiting times, see Table 1 and Proposition 3.1, the construction may lead to a blowup in graph size. Hence, we propose a stochastic variant based on sampling temporal random walks with provable approximation guarantees directly working on the temporal graphs.

Let $\mathbf{G} = (V, \mathbf{E}, l)$ be a temporal graph, the algorithm approximates the normalized feature vector $\phi_{\text{RW}}^k(\mathbf{G}) = \phi_{\text{RW}}^k(\mathbf{G}) / \|\phi_{\text{RW}}^k(\mathbf{G})\|_1$, resulting in the normalized kernel $\hat{\kappa}_{\text{RW}}^k(\mathbf{G}_1, \mathbf{G}_2) = \langle \hat{\phi}_{\text{RW}}^k(\mathbf{G}_1), \hat{\phi}_{\text{RW}}^k(\mathbf{G}_2) \rangle$ for two temporal graphs \mathbf{G}_1 and \mathbf{G}_2 . For simplicity, we only show the approximation for walks of length ex-

actly k , however our results can be easily lifted to approximate walks of length less or equal to k . By Proposition 3.1, this results in an approximation algorithm for the k -step random walk kernel on the directed line graph representation. The algorithm starts by sampling S vertices uniformly at random (with replacement) from V , where the exact cardinality of S will be determined later. For each such vertex, the algorithm performs a temporal random walk w of length k . Finally, we compute a histogram $\tilde{\phi}_{\text{RW}}^k(\mathbf{G})$, where each entry $\tilde{\phi}_{\text{RW}}^k(\mathbf{G})_s$ counts the number of temporal random walks w with $L(w) = s$ encountered during the above procedure, normalized by $1/|S|$. See Algorithm 1 for pseudocode. We

Algorithm 1

Input: A temporal graph \mathbf{G} , a walk length $k > 0$, an additive error term $\lambda > 0$, and a failure probability $\delta < 1$.

Output: A feature vector $\tilde{\phi}_{\text{RW}}^k(\mathbf{G})$ of temporal walk counts.

- 1: Sample S vertices according to Equation (4.1)
 - 2: Initialize feature vector $\tilde{\phi}_{\text{RW}}^k(\mathbf{G})$ to a vector of zeros
 - 3: **parallel for** $s \in S$ **do**
 - 4: Perform temporal random walk w of length k starting at vertex s
 - 5: $\tilde{\phi}_{\text{RW}}^k(\mathbf{G})_{L(w)} \leftarrow \tilde{\phi}_{\text{RW}}^k(\mathbf{G})_{L(w)} + 1/|S|$
 - 6: **end**
 - 7: **return** $\tilde{\phi}_{\text{RW}}^k(\mathbf{G})$
-

get the following result, showing that Algorithm 1 can approximate the normalized (temporal) random-walk kernel $\hat{\kappa}_{\text{RW}}^k(\mathbf{G}_1, \mathbf{G}_2)$ up to an additive error.

THEOREM 4.1. *Let \mathcal{G} be a set of temporal graphs with label alphabet Σ . Moreover let $k > 0$, and let $\Gamma(\Sigma, k)$ denote an upperbound for the number of temporal walks of length k with labels from Σ . By setting*

$$(4.1) \quad S = \frac{\log(2 \cdot |\mathcal{G}| \cdot \Gamma(\Sigma, k) \cdot 1/\delta)}{2(\lambda/\Gamma(\Sigma, h))^2},$$

Algorithm 1 approximates the normalized temporal random walk kernel $\hat{\kappa}_{\text{RW}}^k$ with probability $1 - \delta$, such that

$$\sup_{\mathbf{G}_1, \mathbf{G}_2 \in \mathcal{G}} \left| \hat{\kappa}_{\text{RW}}^k(\mathbf{G}_1, \mathbf{G}_2) - \langle \tilde{\phi}_{\text{RW}}^k(\mathbf{G}_1), \tilde{\phi}_{\text{RW}}^k(\mathbf{G}_2) \rangle \right| \leq 3\lambda.$$

Proof. First, by an application of the Hoeffding together with the Union bound, it follows that by setting

$$S = \frac{\log(2 \cdot |\mathcal{G}| \cdot \Gamma(\Sigma, k) \cdot 1/\delta)}{2\varepsilon^2},$$

it holds that with probability $1 - \delta$,

$$\left| \tilde{\phi}_{\text{RW}}^k(\mathbf{G}_i)_j - \hat{\phi}_{\text{RW}}^k(\mathbf{G}_i)_j \right| \leq \varepsilon,$$

for all j for $1 \leq j \leq \Gamma(\Sigma, k)$, and all temporal graphs \mathbf{G}_i in \mathcal{G} . Let \mathbf{G}_1 and \mathbf{G}_2 in \mathcal{G} , then

$$\begin{aligned} \tilde{\kappa}_{\text{RW}}^k(\mathbf{G}_1, \mathbf{G}_2) &= \left\langle \tilde{\phi}_{\text{RW}}^k(\mathbf{G}_1), \tilde{\phi}_{\text{RW}}^k(\mathbf{G}_2) \right\rangle \\ &\leq \sum_{i=1}^{\Gamma(\Sigma, h)} \left(\tilde{\phi}_{\text{RW}}^k(\mathbf{G}_1)_i \cdot \tilde{\phi}_{\text{RW}}^k(\mathbf{G}_2)_i \right) \\ &\quad + \varepsilon \cdot \sum_{i=1}^{\Gamma(\Sigma, h)} \left(\tilde{\phi}_{\text{RW}}^k(\mathbf{G}_1)_i + \tilde{\phi}_{\text{RW}}^k(\mathbf{G}_2)_i \right) + \sum_{i=1}^{\Gamma(\Sigma, h)} \varepsilon^2 \\ &\leq \hat{\kappa}_{\text{RW}}^k(\mathbf{G}_1, \mathbf{G}_2) + 2\Gamma(\Sigma, h) \cdot \varepsilon + \Gamma(\Sigma, h) \cdot \varepsilon. \end{aligned}$$

The last inequality follows from the fact that the components of $\tilde{\phi}_{\text{RW}}^k(\cdot)$ are in $[0, 1]$. The result then follows by setting $\varepsilon = \lambda/\Gamma(\Sigma, h)$. \square

Notice that our algorithm can be easily modified for the static case and applied to all three of our approaches.

5 Experiments

To evaluate our proposed approaches and investigate their benefits compared to static graph kernels, we address the following questions:

- Q1** How well do our temporal kernels compare to each other and static approaches in terms of (a) accuracy and (b) running time?
- Q2** How does the approximation for the directed line graph approach compare to the exact algorithm?
- Q3** How is the classification accuracy affected by incomplete knowledge of the dissemination process?

5.1 Data Sets We used the following real-world temporal graph data sets representing different types of social interactions.

Infectious and *Highschool*: Two data sets from the *SocioPatterns* project.¹ The *Infectious* graph represents face-to-face contacts between visitors of the exhibition *Infectious: Stay Away* [13]. The *Highschool* graph is a contact network and represents interactions between students in twenty second intervals over seven days.

MIT: A temporal graph of interactions among students of the Massachusetts Institute of Technology [6].

Facebook and *Tumblr*: The first graph is a subset of the activity of the New Orleans Facebook community over three months [33]. The *Tumblr* graph contains quoting between Tumblr users and is a subset of the Memetracker² data set. Rozenstein et al. [29] used these graphs and epidemic simulations to reconstruct dissemination processes.

¹<http://www.sociopatterns.org>

²snap.stanford.edu/data/memetracker9.html

Table 2: Statistics and properties of the data sets.

Properties	Data set					
	MIT	HIGHSCHOOL	INFECTIOUS	TUMBLR	DBLP	FACEBOOK
Size	97	180	200	373	755	995
$\emptyset V $	20	52.3	50	53.1	52.9	95.7
min $ E $	126	286	218	96	206	176
max $ E $	3 363	517	505	190	225	181
$\emptyset E $	702.8	262.4	220.4	98.7	156.8	133.9
$\emptyset \max d(v)$	680.7	92.5	43.8	24.4	26.4	21.0

Table 3: Classification accuracy in percent and standard deviation for the first classification task.

Kernel	Data set						
	MIT	HIGHSCHOOL	INFECTIOUS	TUMBLR	DBLP	FACEBOOK	
Static	<i>Stat-RW</i>	61.03 \pm 2.4	63.94 \pm 2.3	76.40 \pm 1.5	83.68 \pm 1.4	83.75 \pm 0.8	86.43 \pm 0.4
	<i>Stat-WL</i>	42.52 \pm 2.6	45.33 \pm 2.7	68.95 \pm 2.0	78.69 \pm 1.5	78.56 \pm 0.8	83.41 \pm 0.6
Temporal	<i>RD-RW</i>	66.20 \pm 2.6	90.83 \pm 1.3	90.40 \pm 1.0	76.15 \pm 1.5	91.69 \pm 0.5	83.73 \pm 0.8
	<i>RD-WL</i>	83.41 \pm 0.5	90.06 \pm 0.6	91.75 \pm 1.0	70.59 \pm 0.9	90.55 \pm 0.5	82.04 \pm 0.7
	<i>DL-RW</i>	92.91 \pm 0.9	97.39 \pm 0.7	97.95 \pm 0.4	95.15 \pm 0.6	98.86 \pm 0.1	96.46 \pm 0.1
	<i>DL-WL</i>	91.68 \pm 1.6	99.17 \pm 0.6	98.05 \pm 0.4	94.19 \pm 0.4	98.49 \pm 0.2	96.59 \pm 0.2
	<i>SE-RW</i>	88.56 \pm 1.0	96.89 \pm 0.7	97.30 \pm 1.1	95.31 \pm 0.5	98.46 \pm 0.3	95.68 \pm 0.3
	<i>SE-WL</i>	89.52 \pm 1.7	97.56 \pm 0.7	95.40 \pm 0.7	94.13 \pm 1.0	97.23 \pm 0.2	95.26 \pm 0.3
	<i>APPROX (S=50)</i>	82.84 \pm 2.0	87.61 \pm 1.7	83.40 \pm 1.6	89.33 \pm 0.7	93.12 \pm 0.5	89.39 \pm 0.5
	<i>APPROX (S=100)</i>	85.12 \pm 2.6	90.22 \pm 1.9	91.05 \pm 1.0	90.40 \pm 1.0	95.67 \pm 0.5	92.40 \pm 0.4
	<i>APPROX (S=250)</i>	89.30 \pm 2.8	94.00 \pm 1.3	95.05 \pm 0.9	92.74 \pm 0.3	97.22 \pm 0.5	94.64 \pm 0.3

Table 4: Classification accuracy in percent and standard deviation for the second classification task.

Kernel	Data set						
	MIT	HIGHSCHOOL	INFECTIOUS	TUMBLR	DBLP	FACEBOOK	
Static	<i>Stat-RW</i>	57.71 \pm 4.0	62.83 \pm 2.9	66.05 \pm 2.4	67.35 \pm 0.9	60.60 \pm 1.4	67.16 \pm 0.6
	<i>Stat-WL</i>	40.77 \pm 2.5	64.06 \pm 2.4	64.00 \pm 1.3	70.11 \pm 0.5	64.33 \pm 0.8	69.92 \pm 0.3
Temporal	<i>RD-RW</i>	60.57 \pm 4.7	80.06 \pm 1.9	74.00 \pm 1.5	69.54 \pm 1.0	64.24 \pm 1.2	66.35 \pm 0.6
	<i>RD-WL</i>	69.20 \pm 1.8	83.94 \pm 0.7	77.40 \pm 1.2	69.74 \pm 0.5	67.30 \pm 0.5	66.66 \pm 0.6
	<i>DL-RW</i>	82.64 \pm 2.1	93.44 \pm 1.0	88.65 \pm 1.2	77.21 \pm 1.0	81.79 \pm 0.9	79.97 \pm 0.5
	<i>DL-WL</i>	36.40 \pm 4.0	89.33 \pm 0.7	78.65 \pm 1.5	78.18 \pm 1.3	76.45 \pm 1.0	79.99 \pm 0.5
	<i>SE-RW</i>	57.27 \pm 3.3	93.28 \pm 1.3	87.20 \pm 1.1	78.23 \pm 0.9	83.09 \pm 0.6	80.15 \pm 0.6
	<i>SE-WL</i>	50.79 \pm 4.2	91.00 \pm 1.2	79.80 \pm 1.5	80.64 \pm 0.7	82.04 \pm 0.6	75.29 \pm 0.3
	<i>APPROX (S=50)</i>	60.41 \pm 4.0	76.39 \pm 3.0	74.60 \pm 1.8	74.73 \pm 1.3	69.70 \pm 0.8	72.04 \pm 0.7
	<i>APPROX (S=100)</i>	65.41 \pm 4.2	83.83 \pm 1.8	75.60 \pm 1.9	76.49 \pm 1.5	74.50 \pm 0.7	73.08 \pm 0.6
	<i>APPROX (S=250)</i>	66.93 \pm 2.5	90.39 \pm 1.8	78.60 \pm 2.1	78.44 \pm 1.3	76.44 \pm 0.9	77.88 \pm 0.6

DBLP: We used a subset of the DBLP³ database to generate temporal co-author graphs. The subset was chosen by considering publications in proceedings of selected machine learning conferences. The time stamp of an edge is the year of the joint publication.

To obtain data sets for supervised graph classification, we generated induced subgraphs by starting a BFS run from each vertex. We terminated the BFS when at most 20 vertices in case of the MIT, 50 vertices in case of the Infectious, 60 vertices in case of the Highschool, Tumblr or DBLP, and 100 vertices in case of the Facebook graph had been added. Using the above procedure, we generated between 97 and 995 graphs for each of the data sets. See Table 2 for data set statistics.

All data sets will be made publicly available. In the following we describe the model for the dissemination process and the classification tasks.

Dissemination Process Simulation We simulated a dissemination process on each of the induced subgraphs according to the *susceptible-infected (SI)* model—a common approach to simulate epidemic spreading, e.g., see [3]. In the SI model, each vertex is either *susceptible* or *infected*. An infected vertex is part of the temporal dissemination process. An initial seed of s vertices is selected randomly and labeled as infected. Infections propagate in discrete time steps along temporal edges with a fixed probability $0 < p \leq 1$. If a vertex is infected it stays infected indefinitely. A newly infected vertex may infect its neighbors at the next time step. The simulation runs

³<https://dblp.uni-trier.de/>

until at least $|V| \cdot I$ vertices with $0 < I \leq 1$ are infected, or no more infections are possible.

Classification Tasks We consider two classification tasks. The first is the discrimination of temporal graphs with vertex labels corresponding to observations of a dissemination process and temporal graphs in which the labeling is not a result of a dissemination process. Here, for each data set, we run the SI simulation with equal parameters of $s = 1$, $p = 0.5$ and $I = 0.5$ for all graphs. We used half of the data set as our first class. For our second class, we used the remaining graphs. For each graph in the second class, we counted the number V_{inf} of infected vertices, reset the labels of all vertices back to uninfected, and finally infected V_{inf} vertices randomly at a random time.

The second classification task is the discrimination of temporal graphs that differ in the dissemination processes itself. Therefore, we run the SI simulation with different parameters for each of the two subsets. For both subsets we set $s = 1$ and $I = 0.5$. However, for the first subset of graphs we set the infection probability $p = 0.2$ and for the second subset we set $p = 0.8$. The simulation runs repeatedly until at least $|V| \cdot I$ vertices are infected or no more infections are possible. Notice that a classification by only counting the number of infected vertices is impossible for the classification tasks.

In order to evaluate our methods under conditions with incomplete information, we generated additional data sets based on *Infectious* for both classification tasks. For each graph, we randomly set the labels of $\{10\%, \dots, 80\%$ of the infected vertices back to non-infected. We repeated this ten times resulting in 80 data sets for each of the two classification tasks.

5.2 Graph kernels As a baseline we use the k -step random walk (*Stat-RW*) and the Weisfeiler-Lehman subtree (*Stat-WL*) kernel on the static graphs obtained by interpreting the time stamps as discrete edge labels, and assigning to each vertex the concatenated sequence of its labels. To evaluate the three approaches of Section 3, we use the k -step random walk and the Weisfeiler-Lehman subtree kernel, resulting in the following kernel instances: (1) *RD-RW* and *RD-WL*, which use the reduced graph representation (Section 3.1), (2) *DL-RW* and *DL-WL*, which use the directed line graph expansion (Section 3.2), (3) *SE-RW* and *SE-WL*, which use the static expansion (Section 3.3). We evaluate the approximation (*APPROX*) for the directed line graph expansion, proposed in Section 4, with sample sizes $S = 50$, $S = 100$ and $S = 250$.

5.3 Experimental Protocol For each kernel, we computed the normalized Gram matrix. We report the classification accuracies obtained with the C -SVM implementation of LIBSVM [5], using 10-fold cross validation. The C -parameter was selected from $\{10^{-3}, 10^{-2}, \dots, 10^2, 10^3\}$ by 10-fold cross validation on the training folds. We repeated each 10-fold cross validation ten times with different random folds, and report average accuracies and standard deviations. The number of steps of the random walk kernel ($k \in \{0, \dots, 5\}$) and the number of iterations of the Weisfeiler-Lehman subtree kernel ($h \in \{0, \dots, 5\}$) were selected by fold-wise 10-fold cross-validation. All experiments were conducted on a workstation with an Intel Xeon E5-2640v3 with 2.60GHz and 128GB of RAM running Ubuntu 16.04.6 LTS using a single core. We used GNU C++ Compiler 5.5.0 with the flag `-O2`.⁴ To compare running times, we set the walk length of *DL-RW* to $k = 2$, and for *DL-WL* we set the number of iterations to $h = 2$.

5.4 Results and Discussion In the following we answer questions **Q1** to **Q3**.

Q1 Table 3 and Table 4 show that taking temporal information into account is crucial. Our approaches lead to improvements in accuracy over all data sets. In most cases the improvement is substantial. For the first classification task, *DL-RW* and *DL-WL* reach the best accuracies for all but the TUMBLR data set, here *SE-RW* is best. However, also for the other data sets *SE-RW* and *SE-WL* are on par with slightly lower accuracies. For the second classification task, we have a similar situation, our approaches beat the static kernels in all cases. The *Stat-RW* and *Stat-WL* kernels have a significantly lower accuracy for all data sets and are not able to successfully detect dissemination processes. This classification task poses a greater challenge for the temporal kernels which reach less good results compared to the first classification task. Especially the MIT data set seems to be hard, only the *DL-RW* reaches an accuracy of over 80%. However, it also has the overall highest running time for this data set due to its quadratic blowup. See Table 5 for the running times of the first classification task (Table 6 shows similar values for the second task). The running times for the random walk kernels are by orders of magnitude higher than the ones of the Weisfeiler-Lehman kernels. The reduced graph kernels cannot compete with our other approaches in terms of accuracy. In particular for the second classification task the loss of temporal

⁴The code will available at <https://www.github.com>

Table 5: Running times in ms for the first classification task, random walk length $k = 3$ ($k = 2$ for *DL-RW*) and number of iterations of WL $h = 3$ ($h = 2$ for *DL-WL*).

Kernel		Data set					
		MIT	HIGHSCHOOL	INFECTIOUS	TUMBLR	DBLP	FACEBOOK
Stat.	<i>Stat-RW</i>	50330	124060	130630	29209	1090141	456421
	<i>Stat-WL</i>	87	106	129	164	410	715
Temporal	<i>RD-RW</i>	270	4017	10259	14563	99327	357414
	<i>RD-WL</i>	22	84	96	145	405	757
	<i>DL-RW</i>	26447614	33643	10764	2887	6715	5050
	<i>DL-WL</i>	71636	1972	847	429	1242	1131
	<i>SE-RW</i>	7211	3660	4973	2018	6454	5173
	<i>SE-WL</i>	581	382	262	302	1097	1359
	<i>APPROX (S=50)</i>	188	301	309	409	1261	1926
	<i>APPROX (S=100)</i>	363	412	599	944	1982	3452
	<i>APPROX (S=250)</i>	896	1589	1451	1901	5044	7607

Table 6: Running times in ms for the second classification task, random walk length $k = 3$ ($k = 2$ for *DL-RW*) and number of iterations of WL $h = 3$ ($h = 2$ for *DL-WL*).

Kernel		Data set					
		MIT	HIGHSCHOOL	INFECTIOUS	TUMBLR	DBLP	FACEBOOK
Stat.	<i>Stat-RW</i>	48497	107947	139620	32353	1266452	529073
	<i>Stat-WL</i>	73	106	128	164	401	668
Temporal	<i>RD-RW</i>	294	4516	18432	18436	114842	413073
	<i>RD-WL</i>	25	83	98	141	385	729
	<i>DL-RW</i>	26274726	32919	10590	2890	9548	4380
	<i>DL-WL</i>	71180	2121	806	423	1196	1054
	<i>SE-RW</i>	7462	3743	4820	1792	6173	6468
	<i>SE-WL</i>	575	369	261	293	846	1126
	<i>APPROX (S=50)</i>	185	360	305	476	1170	1590
	<i>APPROX (S=100)</i>	361	573	595	807	2318	3696
	<i>APPROX (S=250)</i>	897	1706	1525	1869	5093	7318

information led to lower accuracies. However, the running times, especially of *RD-WL* are low. For a lower average number of temporal edges and vertex degree, its advantage gained by reducing the number of edges decreases, and with larger data sets the running times increase. *RD-RW* and *RD-WL* deliver slightly worse results for the *Facebook* data set compared to the static kernels for both tasks.

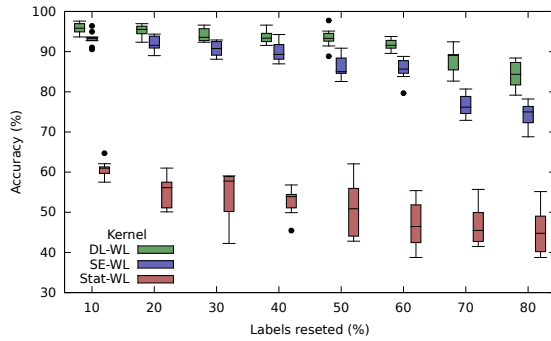
Q2 For a sample size of $S = 50$ *APPROX* performs better than the static kernels. And, the accuracies are on par or better than the ones of the reduced graph kernels. With a larger sample sizes of $S = 100$ and $S = 250$ the gap between the accuracies of *APPROX* and *DL-RW* is reduced for all data sets in both classification tasks. Table 5 shows that the running time of the approximation algorithm is by orders of magnitude faster for the MIT data set. For $S = 50$ and $S = 100$ there is an improvement in running times for all data sets. For $S = 250$ the running times of the exact algorithm for the *Facebook* data set is faster.

Q3 We ran the Weisfeiler-Lehman subtree kernels for the *Infectious* data sets where formerly infected vertices were randomly set to non-infected. For the first classification task *DL-WL* and *SE-WL* keep high

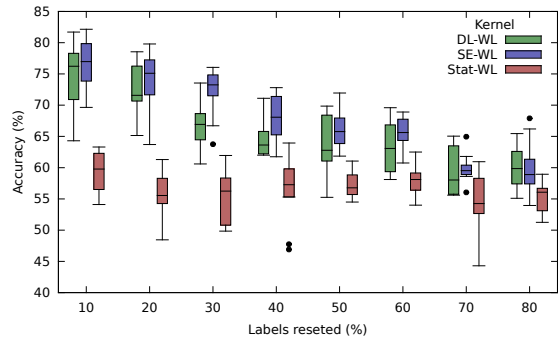
average accuracy, see Figure 3a. The *Stat-WL* kernel falls under 50% accuracy. For the second task the *SE-WL* kernel achieves better average accuracy than the *DL-WL* kernel for up to 70% of reset labels, see Figure 3b. Only for 80% the *DL-WL* kernel achieves better average accuracy.

6 Conclusion

We introduced a framework lifting static kernels to the temporal domain, and obtained variants of the Weisfeiler-Lehman subtree and the k -step random walk kernel. Furthermore, we introduced a stochastic kernel directly based on temporal walks with provable approximation guarantees. We empirically evaluated our methods on real-world social networks showing that incorporating temporal information is crucial for classifying temporal graphs under consideration of dissemination processes. Moreover, we showed that the approximation approach performs well and is able to speed up computation by orders of magnitude. Additionally, we demonstrated that our proposed kernels work in scenarios where information of the dissemination process is incomplete or missing. We believe that our techniques are a stepping stone for developing neural approaches



(a) Results for the first classification task.



(b) Results for the second classification task.

Figure 3: Results of *DL-WL*, *SE-WL* and *Stat-WL* kernel for the *Infectious* data set under incomplete data.

for temporal graph representation learning.

References

- [1] N. Adams and N. Heard. *Dynamic Networks and Cyber-Security*. Imperial College Press, 2016.
- [2] A. Anil, N. Sett, and S. R. Singh. Modeling evolution of a social network using temporal graph kernels. In *ACM SIGIR*, pages 1051–1054, 2014.
- [3] Y. Bai, B. Yang, L. Lin, J. L. Herrera, Z. Du, and P. Holme. Optimizing sentinel surveillance in temporal network epidemiology. *Scientific reports*, 7(1):4804, 2017.
- [4] K. M. Borgwardt and H.-P. Kriegel. Shortest-path kernels on graphs. In *IEEE ICDM*, pages 74–81, 2005.
- [5] C.-C. Chang and C.-J. Lin. LIBSVM: A library for support vector machines. *ACM Transactions on Intelligent Systems and Technology*, 2:27:1–27:27, 2011.
- [6] N. Eagle and A. Pentland. Reality Mining: Sensing complex social systems. *Personal Ubiquitous Computing*, 10(4):255–268, 2006.
- [7] T. Gärtner, P. Flach, and S. Wrobel. On graph kernels: Hardness results and efficient alternatives. In *Learning Theory and Kernel Machines*, pages 129–143, 2003.
- [8] J. Gilmer, S. S. Schoenholz, P. F. Riley, O. Vinyals, and G. E. Dahl. Neural message passing for quantum chemistry. In *ICML*, pages 1263–1272, 2017.
- [9] P. Grindrod, M. C. Parsons, D. J. Higham, and E. Estrada. Communicability across evolving networks. *Physical Review E*, 83(4):046120, 2011.
- [10] F. Harary and R. Z. Norman. Some properties of line digraphs. *Rendiconti del Circolo Matematico di Palermo*, 9(2):161–168, May 1960.
- [11] P. Holme. Epidemiologically optimal static networks from temporal network data. *PLoS computational biology*, 9(7):e1003142, 2013.
- [12] P. Holme. Modern temporal network theory: a colloquium. *The European Physical Journal B*, 88(9):234, 2015.
- [13] L. Isella, J. Stehlé, A. Barrat, C. Cattuto, J.-F. Pinton, and W. Van den Broeck. What’s in a crowd? Analysis of face-to-face behavioral networks. *Journal of Theoretical Biology*, 271(1):166–180, 2011.
- [14] K. Knauf, D. Memmert, and U. Brefeld. Spatio-temporal convolution kernels. *Machine Learning*, 102(2):247–273, Feb 2016.
- [15] R. Kondor and H. Pan. The multiscale Laplacian graph kernel. In *NIPS*, pages 2982–2990, 2016.
- [16] N. M. Kriege, P.-L. Giscard, and R. C. Wilson. On valid optimal assignment kernels and applications to graph classification. In *NIPS*, pages 1615–1623, 2016.
- [17] N. M. Kriege, F. D. Johansson, and C. Morris. A survey on graph kernels. *CoRR*, abs/1903.11835, 2019.
- [18] N. M. Kriege, M. Neumann, C. Morris, K. Kersting, and P. Mutzel. A unifying view of explicit and implicit feature maps for structured data: Systematic studies of graph kernels. *CoRR*, abs/1703.00676, 2017.
- [19] J. Leskovec, A. Krause, C. Guestrin, C. Faloutsos, C. Faloutsos, J. VanBriesen, and N. Glance. Cost-effective outbreak detection in networks. In *ACM KDD 2007*, pages 420–429. ACM, 2007.
- [20] L. Li, H. Tong, Y. Xiao, and W. Fan. *Cheetah*: Fast graph kernel tracking on dynamic graphs. In *SDM*, pages 280–288, 2015.
- [21] O. Michail. An introduction to temporal graphs: An algorithmic perspective. *Internet Mathematics*, 12(4):239–280, 2016.
- [22] O. Michail and P. G. Spirakis. Traveling salesman problems in temporal graphs. *Theoretical Computer Science*, 634:1–23, 2016.
- [23] C. Morris, K. Kersting, and P. Mutzel. Glocalised Weisfeiler-Lehman kernels: Global-local feature maps of graphs. In *IEEE ICDM*, pages 327–336, 2017.
- [24] C. Morris, M. Ritzert, M. Fey, W. L. Hamilton, J. E. Lenssen, G. Rattan, and M. Grohe. Weisfeiler and Leman go neural: Higher-order graph neural networks. In *AAAI Conference on Artificial Intelligence*, volume 33, pages 4602–4609, 2019.
- [25] G. H. Nguyen, J. B. Lee, R. A. Rossi, N. K. Ahmed, E. Koh, and S. Kim. Continuous-time dynamic network embeddings. In *The Web Conference*, pages 969–976, 2018.
- [26] G. Nikolentzos, P. Meladianos, S. Limmios, and

- M. Vazirgiannis. A degeneracy framework for graph similarity. In *IJCAI*, pages 2595–2601, 2018.
- [27] G. Nikolentzos, P. Meladianos, and M. Vazirgiannis. Matching node embeddings for graph similarity. In *AAAI*, pages 2429–2435, 2017.
- [28] B. Paaßen, C. Göpfert, and B. Hammer. Time series prediction for graphs in kernel and dissimilarity spaces. *Neural Processing Letters*, pages 1–21, 2017.
- [29] P. Rozenshtein, A. Gionis, B. A. Prakash, and J. Vreeken. Reconstructing an epidemic over time. In *ACM KDD*, pages 1835–1844. ACM, 2016.
- [30] N. Shervashidze, P. Schweitzer, E. J. van Leeuwen, K. Mehlhorn, and K. M. Borgwardt. Weisfeiler-Lehman graph kernels. *Journal of Machine Learning Research*, 12:2539–2561, 2011.
- [31] M. Sugiyama and K. M. Borgwardt. Halting in random walk kernels. In *NIPS*, pages 1639–1647, 2015.
- [32] R. Trivedi, M. Farajtabar, P. Biswal, and H. Zha. Dyrep: Learning representations over dynamic graphs. In *ICLR*, 2019.
- [33] B. Viswanath, A. Mislove, M. Cha, and K. P. Gummadi. On the evolution of user interaction in facebook. In *ACM Workshop on Online Social Networks*, pages 37–42, 2009.
- [34] S. Vosoughi, D. Roy, and S. Aral. The spread of true and false news online. *Science*, 359(6380):1146–1151, 2018.
- [35] H. Wang, J. Wu, X. Zhu, Y. Chen, and C. Zhang. Time-variant graph classification. *IEEE Transactions on Systems, Man, and Cybernetics: Systems*, 2018.
- [36] World Health Organization (WHO). Ebola virus disease, democratic republic of the congo, external situation report 43. 2019.
- [37] B. Wu, C. Yuan, and W. Hu. Human action recognition based on context-dependent graph kernels. In *IEEE CVPR*, pages 2609–2616, 2014.